Cell Reports
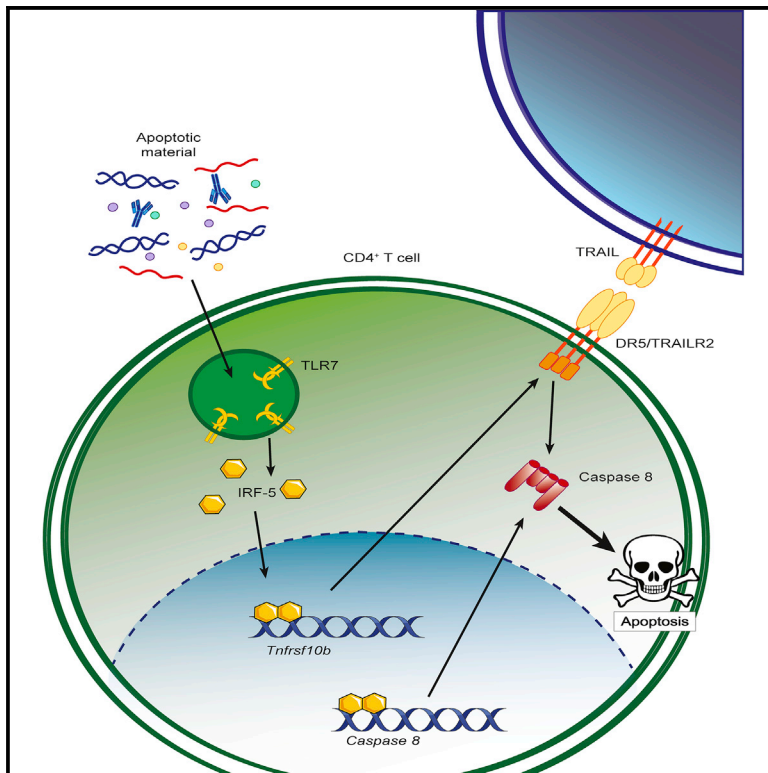
IRF-5 Promotes Cell Death in CD4 T Cells during Chronic Infection

Graphical Abstract

Authors

Aymeric Fabié, Linh Thuy Mai,
Xavier Dagenais-Lussier, Akil Hammami,
Julien van Grevenynghe, Simona Stäger

Correspondence

simona.stager@iaf.inrs.ca

In Brief

Fabié et al. report a role for IRF-5 in IFNγ^+ CD4 T cell death during chronic visceral leishmaniasis. IRF-5 is activated by apoptotic cell material, derived from inflammatory tissue damage, via TLR7, resulting in upregulation of death receptor 5 and caspase 8 and cell death of protective CD4 T cells.

Highlights

- Apoptotic cell material triggers TLR7 in IFNγ^+ CD4 T cells during chronic infection

- Signaling via TLR7 induces the upregulation and activation of IRF-5 in CD4 T cells

- IRF-5 promotes the upregulation of DR5 and caspase 8

- Inflammatory tissue damage sensitizes protective CD4 T cells to cell death

CellPress

IRF-5 Promotes Cell Death in CD4 T Cells during Chronic Infection

Aymeric Fabié,[1] Linh Thuy Mai,[1] Xavier Dagenais-Lussier,[1] Akil Hammami,[1] Julien van Grevenynghe,[1] and Simona Stäger[1,2,*]
[1]INRS-Institut Armand-Frappier, 531 Boulevard des Prairies, Laval, QC H7V 1B7, Canada
[2]Lead Contact
*Correspondence: simona.stager@iaf.inrs.ca
https://doi.org/10.1016/j.celrep.2018.06.107

SUMMARY

The transcription factor interferon regulatory factor 5 (IRF-5) plays an important function in innate immunity and in initiating pro-inflammatory responses against pathogens. IRF-5 is constitutively expressed in several cell types, including plasmacytoid dendritic cells, monocytes, and B cells. We have previously reported that IRF-5 is also expressed in T cells during infection. The role of IRF-5 in T cells is yet unknown. Here, we demonstrate that IRF-5 is increasingly expressed in interferon (IFN)-γ^+ CD4 T cells over the course of *L. donovani* infection. This transcription factor is induced by apoptotic material via Toll-like receptor 7 (TLR7) and promotes the expression of death receptor 5 (DR5). IRF-5 activation sensitizes CD4 T cells to cell death. Because tissue disruption and chronic inflammation are common characteristics of persistent infections, activation of IRF-5 in CD4 T cells may represent a common pathway that leads to suppression of protective CD4 T cell responses, favoring the establishment of chronic infection.

INTRODUCTION

The transcription factor interferon regulatory factor 5 (IRF-5) has been implicated in the antiviral immune response because of its involvement in the transcriptional activation of both type I interferon (IFN) genes and genes encoding key pro-inflammatory cytokines in antigen-presenting cells (Barnes et al., 2001, 2004; Takaoka et al., 2005). Besides its important role in innate immunity, IRF-5 also appears to be a critical regulator of DNA-damage-induced apoptosis and tumor suppression (Bi et al., 2014; Couzinet et al., 2008). In human, various *IRF5* polymorphisms are also linked to autoimmune diseases, including lupus erythematosus (Graham et al., 2006), rheumatoid arthritis (Dieguez-Gonzalez et al., 2008), and inflammatory bowel disease (Dideberg et al., 2007). IRF-5 is constitutively expressed by several cell types, such as plasmacytoid dendritic cells, monocytes, and B cells. Activation of IRF-5 occurs after phosphorylation, following which this transcription factor delocalizes from
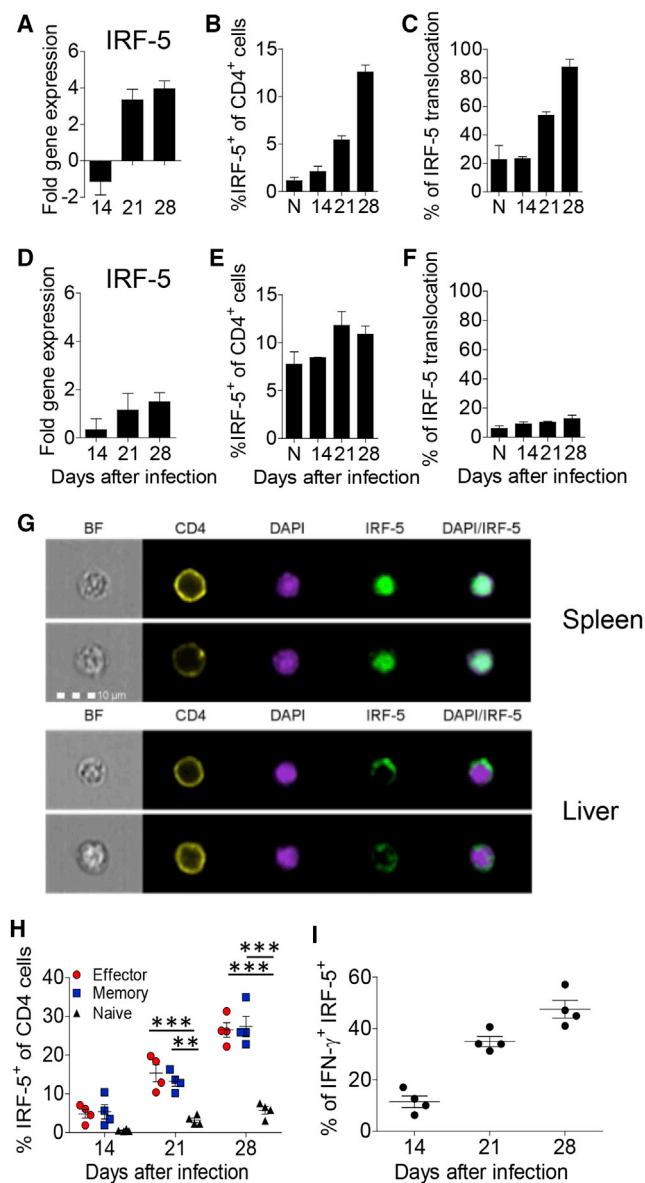
the cytoplasm to the nucleus. IRF-5 can be activated by Toll-like receptor 7 (TLR7) and TLR9 via the MyD88 signaling pathway, directly by viral infections and type I IFN (Schoenemeyer et al., 2005), or by apoptotic and/or necrotic material (Stone et al., 2012).

Visceral leishmaniasis (VL) is a potentially lethal chronic disease that causes hepatosplenomegaly, anemia, cachexia, hypergammaglobulinemia, and immunosuppression (Kaye et al., 2004). Mice infected with the protozoan parasite *Leishmania donovani*, a causative agent of VL, also develop hepatosplenomegaly (Kaye et al., 2004). Although infection in the liver is self-resolving, the parasite persists in the spleen of infected mice. Chronic infection in the spleen is associated with disruption of the splenic architecture and massive recruitment of pro-inflammatory cells. IFN-γ-producing CD4 T cell responses are essential for controlling parasite growth but only develop 2 to 3 weeks after infection and gradually show signs of functional exhaustion soon thereafter. CD8 T cells also contribute to protection; however, these cells undergo very limited expansion and become dysfunctional during chronic infection (Hammami et al., 2015; Joshi et al., 2009). Protective T cell responses are also suppressed by interleukin-10 (IL-10) derived from IFN-γ^+IL-10$^+$ CD4 T cells (Ranatunga et al., 2009; Stäger et al., 2006) and B cells (Bankoti et al., 2012) and by myeloid-derived suppressor cells (Hammami et al., 2017).

We have previously reported that *Irf5$^{-/-}$* mice are more susceptible to *L. donovani* infection. Susceptibility was associated with a significant reduction of inflammatory cell infiltration in the liver and spleen and with a severe impairment in the development of Th1 cells (Hammami et al., 2015; Paun et al., 2011). IRF-5 was indeed required for inducing IL-12 production by dendritic cells and sustaining Th1 responses. Our results were in agreement with Krausgruber et al. (2011), who demonstrated the critical role of this transcription factor in determining lineage commitment of inflammatory macrophages by promoting IL-12 while repressing IL-10. Interestingly, we noticed that IRF-5 mRNA was also upregulated in total splenic T cells mainly during chronic infection (Paun et al., 2011). The role of IRF-5 in T cells is yet unknown.

Here, we show that IRF-5 is upregulated and activated in CD4 T cells during chronic VL. This transcription factor is induced by TLR7 triggering. IRF-5 activation results in the upregulation of death receptor 5 (DR5) and, ultimately, in CD4 T cell death.

Figure 1. IRF-5 Is Activated in Splenic CD4 T Cells during Chronic Visceral Leishmaniasis

Mice were infected with 2×10^7 amastigotes intravenously and euthanized at various time points after infection.

(A) Real-time PCR analysis of splenic CD4 T cells from *L. donovani*-infected mice measuring mRNA for IRF5.

(B) Percentage of splenic CD4 T cells expressing IRF5 after *L. donovani* infection.

(C) Percentage of IRF5 nuclear translocation in splenic CD4 T cells.

(D) Real-time PCR analysis of IRF-5 mRNA expression levels in hepatic CD4 T cells.

(E and F) Percentage of hepatic CD4 T cells expressing IRF5 (E) and percentage of hepatic CD4 T cells showing IRF5 nuclear translocation (F).

(G) Representative images of CD4 T cells expressing IRF5: CD4 (yellow); nucleus (purple); and IRF5 (green). The last column represents co-expression of nuclear staining and IRF5. Upper row: examples of IRF-5 nuclear localization in spleen are shown; lower row: examples of cytoplasmic localization in liver are shown.

(H) Percentage of splenic effector (CD44+ CD62L−), memory (CD44+ CD62L+), and naive (CD44− CD62L+) CD4 T cells expressing IRF5 over the course of infection.

RESULTS

IRF-5 Is Activated in Splenic CD4 T Cells during Chronic VL

We have previously reported that IRF-5 mRNA is expressed in splenic T cells in *L. donovani*-infected mice (Paun et al., 2011). Because effector CD8 T cells are not functional (Hammami et al., 2015; Joshi et al., 2009) and do not express IRF-5 during chronic VL (data not shown), we decided to concentrate our analysis on CD4 T cells. Splenic CD4 T cells upregulated IRF-5 mRNA from day 21 (d21) post infection (p.i.) on (Figure 1A). Image Stream flow cytometry analysis revealed that about 5%–12% of splenic CD4 T cells expressed IRF-5 on the protein level (Figure 1B) and that this transcription factor was increasingly translocated to the nucleus over the course of infection (Figures 1C, 1G [upper rows], S1A, and S1B), indicating that it was activated. Although a significant percentage of CD4 T cells expressed IRF-5 in the liver (Figures 1D and 1E), this transcription factor remained in the cytoplasm and was not translocated to the nucleus (Figures 1F, 1G [lower rows], S1A, and S1B). Next, we wanted to identify splenic CD4 T cell subpopulations expressing IRF-5. As shown in Figure 1H, effector and memory cells, but not naive CD4 T cells, were positive for IRF-5 during chronic VL (Figure S1C). A closer analysis of subpopulations expressing IRF-5 revealed that 40%–50% of IFN-γ-producing CD4 T cells were expressing this transcription factor at d21 and d28 p.i. (Figure 1I). Hence, IRF-5 appears to be active in splenic, but not hepatic, IFN-γ-producing CD4 T cells during chronic *L. donovani* infection.
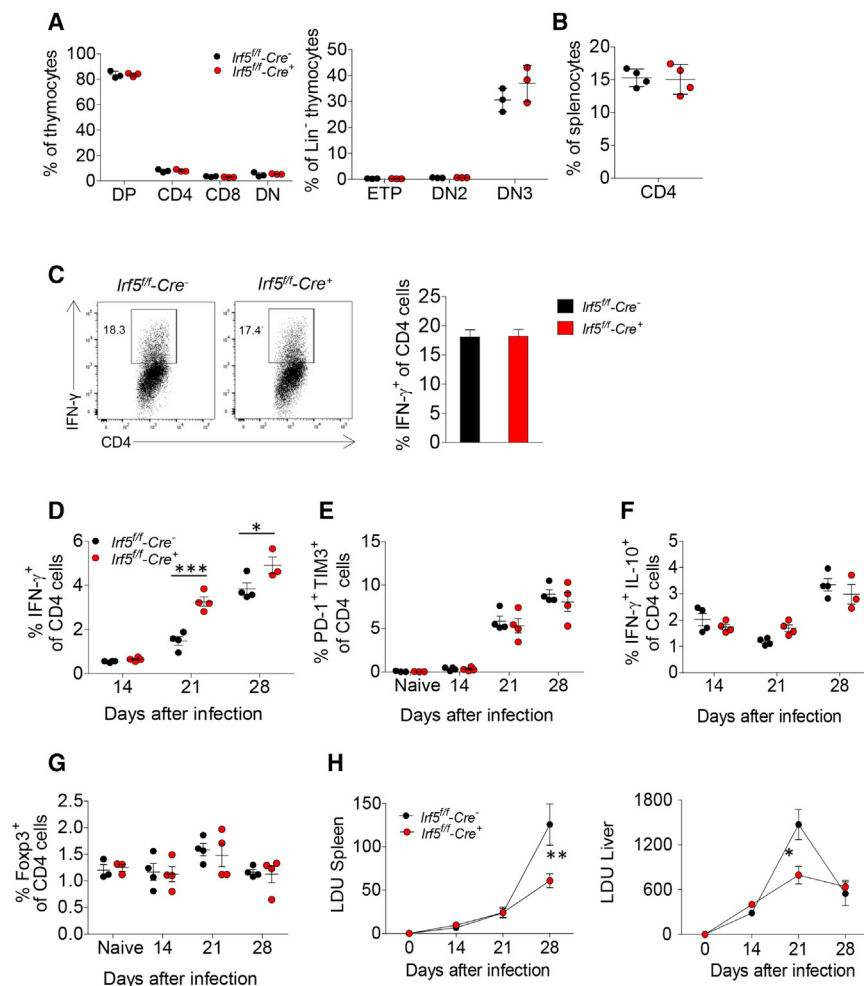
Cell-Specific IRF-5 Ablation in T Cells Results in Higher Frequencies of IFN-γ-Producing CD4 T Cells during VL

To better characterize the function of IRF-5 in CD4 T cells, we generated T-cell-specific *Irf5*$^{−/−}$ mice. We first compared the frequency of CD4 T cells and T cell precursors in the thymus of naive *Irf5*$^{flox/flox}$-*Cre*$^+$ (IRF-5 deficient) to that of *Cre*$^−$ (IRF-5 sufficient) littermate controls to ensure that the absence of IRF-5 did not alter T cell development. The percentage of various precursors and of CD4 T cells present in the thymus was comparable in both groups of mice (Figures 2A, S2A, and S2B), as was the frequency of CD4 T cells in the spleen (Figures 2B and S2C). This confirmed that T cell development was normal in our T-cell-specific IRF-5-deficient mice and that we could use these mice to investigate IRF-5 function in T cells during VL. Because total *Irf5*$^{−/−}$ mice develop defective Th1 responses following *L. donovani* infection (Paun et al., 2011), we sought to determine whether this transcription factor was required for IFN-γ production by CD4 T cells. Hence, we stimulated naive CD4 T cells from *Cre*$^+$ and *Cre*$^−$ mice with anti-CD3/CD28 in the presence of recombinant IL-12 and monitored IFN-γ production. The absence of IRF-5 did not seem to affect the differentiation into IFN-γ-producing Th1 cells (Figure 2C), suggesting that defective Th1 responses in *L. donovani*-infected total *Irf5*$^{−/−}$ mice was more a

(I) Percentage of IRF-5$^+$ within the IFN-γ$^+$ CD4 T population.

Data represent mean ± SEM of one of 3 or 4 independent experiments; n = 3–5.
**p < 0.01; ***p < 0.001.

Figure 2. Cell-Specific IRF-5 Ablation in T Cells Results in Higher Frequencies of IFN-γ-Producing CD4 T Cells during VL

Thymus and spleen from naive $Irf5^{f/f}$-Cre^- and $Irf5^{f/f}$-Cre^+ mice were harvested to assess T cells development.

(A) Percentage of thymic T cells in $Irf5^{f/f}$-Cre^- and $Irf5^{f/f}$-Cre^+ mice, showing CD4$^+$CD8$^+$ double positive (DP), CD4$^+$ or CD8$^+$ single positive, and CD4$^-$ CD8$^-$ double negative (DN) cells (left panel). T cell progenitors were first gated on Lin$^-$ lineage negative (B220, CD3ε, CD11b, GR1, Ter119, and CD8α) and then separated according to c-Kit (CD117) and CD25 expression as follows: c-Kit$^+$ CD25$^-$ ETP; c-Kit$^+$ CD25$^+$ DN2; and c-Kit$^-$ CD25$^+$ DN3 (right panel).

(B) Percentage of splenic CD4 T cells in naive $Irf5^{f/f}$-Cre^- and $Irf5^{f/f}$-Cre^+ mice.

(C) CD4$^+$ T cells from $Irf5^{f/f}$-Cre^- and $Irf5^{f/f}$-Cre^+ mice were stimulated with anti-CD3/CD28 in the presence of IL-12. Representative FACS plots and percentage of IFN-γ$^+$ CD4 T cells are shown.

(D–G) Mice were infected with 2 × 10^7 amastigotes intravenously and euthanized at various time points after infection. Graphs show frequency of (D) IFN-γ$^+$CD3$^+$ CD4$^+$, (E) PD-1$^+$ TIM3$^+$CD3$^+$ CD4$^+$, (F) IFN-γ$^+$ IL-10$^+$CD3$^+$ CD4$^+$, and (G) FoxP3$^+$CD3$^+$ CD4$^+$ T cells in infected $Irf5^{f/f}$-Cre^- and $Irf5^{f/f}$-Cre^+ mice.

(H) Graphs represent the splenic (left) and hepatic (right) parasite burden at different times of $L.$ $donovani$ infection.

Data are shown as the mean ± SEM of one of 3 independent experiments; n = 3–5. *p < 0.05; **p < 0.01; ***p < 0.001.
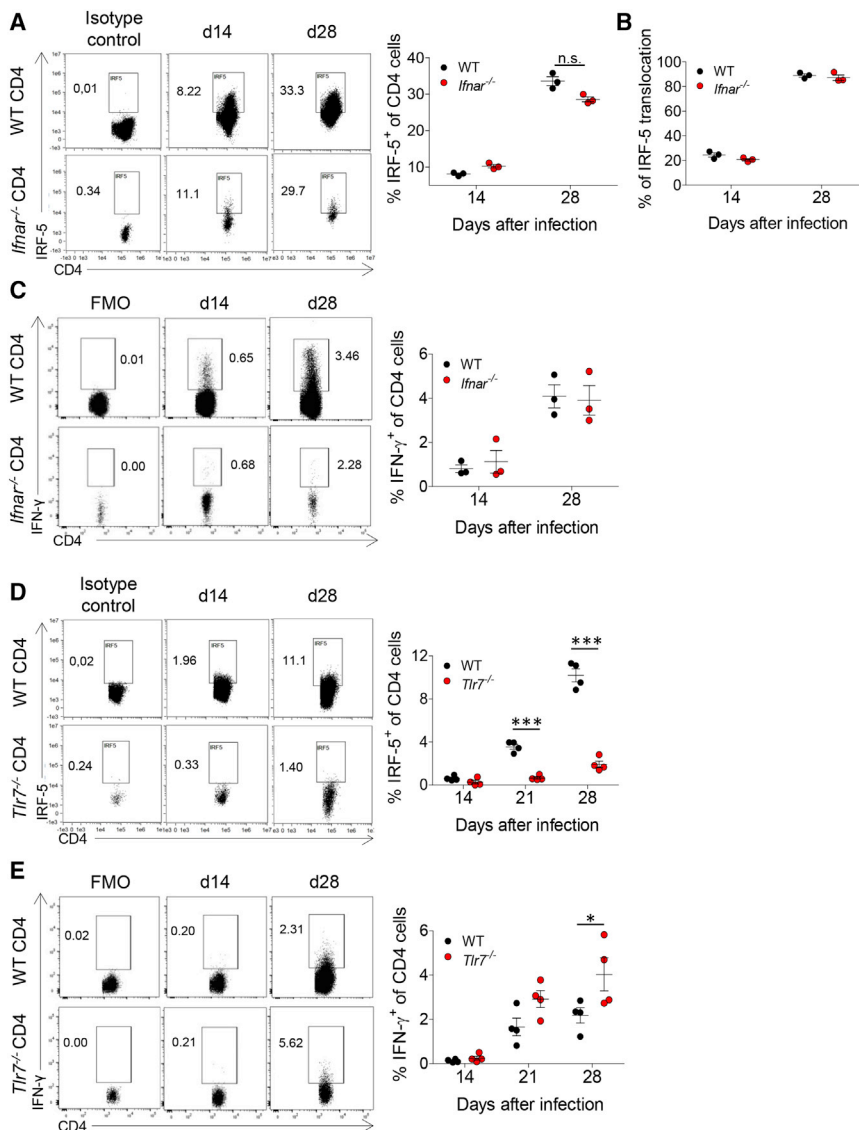
consequence of antigen-presenting cell (APC) malfunction rather than an intrinsic T cell effect, in agreement with Krausgruber et al. (2011).

We then infected Cre^+ and Cre^- mice with $L.$ $donovani$ and monitored CD4 T cell responses over the course of infection. Interestingly, similar frequencies of splenic IFN-γ$^+$ CD4 T cells were detected in both groups of mice at d14 p.i.; however, at d21 and d28 p.i., IFN-γ-producing CD4 T cells were significantly more abundant in the spleen of T-cell-specific $Irf5^{-/-}$ mice (Figures 2D and S2D). We next investigated whether this increase was a consequence of fewer CD4 T cells becoming exhausted during chronic VL. The frequency of exhausted PD-1$^+$ TIM3$^+$ CD4 T cells did not vary between both groups of infected mice (Figure 2E). To rule out the possibility that IRF-5 was affecting the survival of regulatory T cells and that this had an indirect impact on the frequencies of IFN-γ$^+$ CD4 T cells, we examined Tr1 and Tregs responses. No differences were observed in the percentage of IFN-γ$^+$ IL-10$^+$ Tr1 cells (Stäger et al., 2006; Figure 2F) or Foxp3$^+$ CD4 T cells (Figures 2G and S2D), concurring with our previous observation that IRF-5 was mainly active in IFN-γ$^+$ CD4 T cells. Overall, these results indicate that IRF-5 may be involved in regulating the survival of IFN-γ$^+$ CD4 T cells.

Because Th1 responses are required to control parasite growth (Bankoti and Stäger, 2012), it was not surprising that Cre^+ mice displayed a significantly lower splenic and hepatic parasite burden (Figure 2H).

TLR7 Is Required to Induce IRF-5 in CD4 T Cells during VL

In the following experiment, we wanted to identify which pathway was responsible for IRF-5 upregulation in IFN-γ$^+$ CD4 T cells to better understand the role this transcription factor might have in these cells. IRF-5 can be induced, among others, by IFN-I and TLR7. IFN-I is upregulated during chronic VL (Silva-Barrios et al., 2016), and TLR7 can be triggered by the parasite (Paun et al., 2011; Silva-Barrios et al., 2016). Hence, we performed adoptive transfer experiments using $Ifnar^{-/-}$ and $Tlr7^{-/-}$ CD4 T cells and monitored the expression of IRF-5 in endogenous and adoptively transferred cells during the course of $L.$ $donovani$ infection. When we transferred $Ifnar^{-/-}$ CD4 T cells into congenic mice, we noticed that IRF-5 was upregulated (Figure 3A) and translocated (Figure 3B) at similar levels as endogenous wild-type (WT) CD4 T cells. Moreover, no differences were observed in the percentage of

Figure 3. TLR7 Is Required to Induce IRF-5 in CD4 T Cells during VL

CD4 T cells from $Ifnar^{-/-}$ and $Tlr7^{-/-}$ mice were adoptively transferred into CD45.1 congenic mice a day prior to infection with 2×10^7 *L. donovani* amastigotes.

(A–C) Graphs show (A) the percentage of endogenous (WT) and adoptively transferred ($Ifnar^{-/-}$) CD4 T cells expressing IRF5, (B) the percentage of IRF5 nuclear translocation, and (C) the frequency of splenic IFN-γ⁺ CD3⁺ CD4⁺ T cells over the course of *L. donovani* infection.

(D and E) Graphs represent (D) the percentage of endogenous (WT) and adoptively transferred ($Tlr7^{-/-}$) CD4 T expressing IRF5 and (E) the percentage of splenic IFN-γ⁺ CD3⁺ CD4⁺ T cells over the course of *L. donovani* infection.

Data are shown as the mean ± SEM of one of 3 independent experiments; n = 3–4. *p < 0.05; ***p < 0.001.

IFN-γ-producing cells between WT and $Ifnar^{-/-}$ CD4 T cells (Figure 3C). In contrast, adoptively transferred $Tlr7^{-/-}$ CD4 T cells failed to upregulate IRF-5 (Figure 3D), suggesting that TLR7 is upstream of IRF-5 in CD4 T cells. Similarly to $Irf5^{-/-}$ cells (Figure 2D), significantly more $Tlr7^{-/-}$ CD4 T cells expressed IFN-γ at d28 p.i. (Figure 3E).

TLR7-Induced IRF-5 Promotes the Upregulation of DR5 and Induces Cell Death in CD4 T Cells from *L. donovani*-Infected Mice
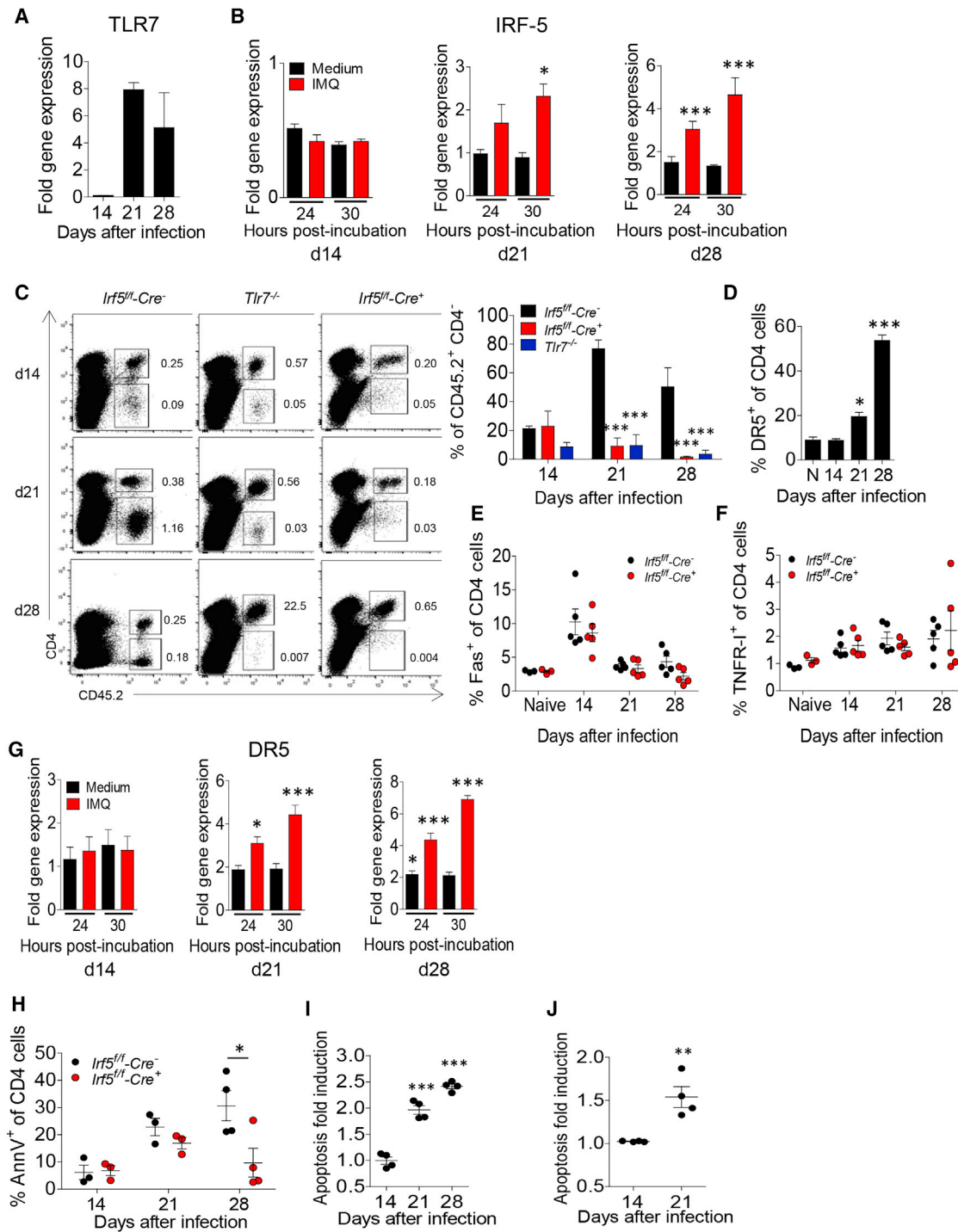
Several studies have reported the expression of various TLRs, including TLR7, on murine T cell subsets (Caramalho et al., 2003; Fukata et al., 2008; Gelman et al., 2004; Tomita et al., 2008). To better identify the role of TLR7 in inducing IRF-5, we first assessed its expression on CD4 T cells over the course of *L. donovani* infection. The expression kinetics of TLR7 mRNA was similar to the one observed for IRF-5: at d14 p.i., it was ex-

pressed at similar levels as in CD4 T cells from naive mice; however, by d21 and d28 p.i., CD4 T cells from infected mice significantly upregulated TLR7 (Figure 4A). We next investigated whether TLR7 was responsible for IRF-5 induction in CD4 T cells during VL. CD4 T cells were purified from the spleen of *L. donovani*-infected mice at d14, d21, and d28 p.i. and treated *in vitro* with the TLR7 agonist imiquimod (IMQ). IRF-5 mRNA expression was evaluated 24 and 30 hr after stimulation (Figure 4B). As expected, treatment with IMQ did not induce IRF-5 in CD4 T cells purified from the spleen at d14 p.i., because the cells do not yet express TLR7 (Figure 4B). In contrast, when we stimulated cells enriched at d21 and d28 p.i., we saw an upregulation of IRF-5 at 24 and 30 hr post-treatment (Figure 4B).

When we perform adoptive transfer experiments using CD4 T cells, we notice that a large percentage of adoptively transferred wild-type CD4 T cells downregulates CD4 (Figure 4C). About 70% (at d21) and 50% (at d28) of the adoptively transferred CD4 T cells present in the spleen are CD4$^{lo/neg}$. Most of these cells also downregulated CD3 (Figure S3A), and about 30% of the cells were DR5 and annexin V positive (Figures S3B and S3C). Interestingly, the majority of the CD4$^{lo/neg}$ T cells upregulated B220 (Figure S3D), a marker that has been associated with pre-apoptotic stages in T cells (Oka et al., 2000; Park et al., 2002; Renno et al., 1998).

Surprisingly, adoptive transfer of $Tlr7^{-/-}$ or $Irf5^{-/-}$ CD4 T cells does not lead to the same results and only a small percentage of cells downregulate CD4 at d21 and d28 p.i. (Figure 4C).

IRF-5 has been described to transcriptionally regulate death receptor 5 (DR5 or TRAIL receptor 2) in human colorectal carcinoma cell lines, sensitizing cells to TRAIL-induced apoptosis

Figure 4. TLR7-Induced IRF-5 Promotes the Upregulation of DR5 and Induces Cell Death in CD4 T Cells from *L. donovani*-Infected Mice

Mice were infected with 2×10^7 amastigotes intravenously and euthanized at various time points after infection.

(A) Real-time PCR of splenic CD4 T cells from infected mice measuring mRNA for TLR7.

(B) Purified CD4 T cells from infected mice were incubated with medium or imiquimod. Real-time PCR analysis of IRF5 mRNA levels in CD4 T cells from infected C57BL/6 mice.

(C) *Irf5^{f/f}-Cre^+*, *Irf5^{f/f}-Cre^−*, and *Tlr7^{−/−}* CD4 T cells were adoptively transferred into congenic CD45.1 mice a day prior to *L. donovani* infection. Representative dot plots (left panels) and percentages (right panel) of adoptively transferred CD45.2^+ cells from the various donors are shown.

(D–I) Mice were infected with 2×10^7 amastigotes intravenously and euthanized at various time points after infection. Graphs show frequency of (D) DR5^+, (E) Fas^+, and (F) TNFR-I^+ CD4 T cells in the spleen of naive and *L. donovani*-infected mice.

(legend continued on next page)

(Hu and Barnes, 2009). Thus, we were wondering whether DR5 and cell death were also promoted following TLR7 stimulation of CD4 T cells. We first assessed whether DR5 was expressed on CD4 T cells during VL, and we noticed that this molecule was upregulated on CD4 T cells from d21 p.i. on (Figures 4D and S4A). We also monitored the expression of Fas receptor (FasR), another known IRF-5 target (Hu and Barnes, 2009), on CD4 T cells from *L. donovani*-infected *Irf5*^*flox/flox*^-*Cre*^+^ and *Cre*^−^ mice. No differences were observed between *Cre*^+^ and *Cre*^−^ mice (Figures 4E and S4B). Similar results were obtained when we assessed tumor necrosis factor (TNF) receptor-I (TNFR-I) expression (Figures 4F, S4C, and S4D), suggesting that DR5, but not FasR or TNFR-I, may possibly be a target of IRF-5 in CD4 T cells.

Indeed, DR5 was also upregulated on CD4 T cells purified at d21 and d28 p.i., but not on those from d14 p.i. following TLR7 stimulation with IMQ (Figure 4G), implying that the TLR7-IRF-5-DR5 pathway could predispose CD4 T cells to cell death. Hence, we monitored the expression of annexin V on CD4 T cells in *L. donovani*-infected *Cre*^+^ and *Cre*^−^ mice (Figures 4H and S4E). CD4 T cells in IRF-5-sufficient mice increasingly showed signs of apoptosis over the course of VL, and the frequency of CD4 T cells expressing annexin V was significantly lower at d28 p.i. in *Cre*^+^ mice. Moreover, apoptosis was also induced in CD4 T cells purified at d21 and d28 p.i. following incubation with IMQ (Figure 4I), although annexin V expression was not altered in CD4 T cells from d14-p.i.-infected mice. To determine whether IRF-5 induction in CD4 T cells made cells more prone to TRAIL-mediated death, we treated CD4 T cells purified at d14 and d21 p.i. from *L. donovani*-infected mice with recombinant TRAIL. Cell death was assessed after 6 hr by fluorescence-activated cell sorting (FACS). As shown in Figure 4J, treatment with recombinant TRAIL (rTRAIL) did not alter cell survival rate in CD4 purified at d14 p.i. when DR5 is still expressed at low levels (Figure 4D). In contrast, when we incubated CD4 T cells from d21-infected mice, we noticed a significant increase in cell death in rTRAIL-treated cells.

Taken together, these results indicate that the TLR7-IRF-5-DR5 axis sensitizes splenic CD4 T cells to TRAIL-induced cell death during VL.

IRF-5 Does Not Affect CD4 T Cell Proliferation

IRF-5 was reported to be involved in cell cycle regulation in tumor cells (Barnes et al., 2003). Thus, we assessed whether there was a difference in the proliferative capacity between *Cre*^−^ and *Cre*^+^ CD4 T cells. Carboxyfluorescein succinimidyl ester (CFSE)-labeled naive *Cre*^−^ and *Cre*^+^ CD4 T cells were stimulated with anti-CD3/CD28 *in vitro* for 5 days. No differences in the percentage of CFSE^lo/int^ cells were observed between the two groups over the 5-day period (Figure 5A), indicating that IRF-5 deficiency did not confer a proliferative advantage. To test whether *Cre*^−^ and *Cre*^+^ CD4 T cells had similar proliferative capacities during *L. donovani* infection, we performed a double adoptive transfer experiment, in which IRF-5-sufficient CD45.1 and IRF-5-deficient CD45.2 CD4 T cells were co-transferred into CD45.1/CD45.2 recipients a day prior to *L. donovani* infection. The proliferative capacity was monitored based on the Ki67 expression. As shown in Figure 5B, IRF-5-sufficient and deficient cells had similar Ki67 expression levels, suggesting that the absence of IRF-5 did not alter cell division in CD4 T cells *in vivo* as well. Interestingly, though, the number of IRF-5-deficient CD4 T cells present in the spleen at d21 and d28 p.i. was significantly higher than that of IRF-5-sufficient cells (Figure 5C). Because both cell types had similar proliferative capacities (Figure 5B), this implies that wild-type CD4 T cells were dying.

TLR7-Mediated IRF-5 Activation and CD4 Cell Death Are Not a Consequence of Microbial Sensing

The next important question that arose was to determine whether TLR7 on CD4 T cells was directly triggered by *L. donovani* and whether other pathways were also involved in inducing IRF-5. Hence, we incubated CD4 T cells purified from d14, d21, and d28 p.i. with CpG, lipopolysaccharide (LPS), parasites, and parasite RNA or DNA and monitored IRF-5 and DR5 expression by flow cytometry. Because apoptotic and/or necrotic material has also been described to induce IRF-5 in monocytes of systemic lupus erythematosus (SLE) patients (Stone et al., 2012) and splenic tissue disruption occurs during chronic VL (Smelt et al., 1997), we incubated CD4 T cells with supernatant (SN) of apoptotic splenocytes previously incubated with staurosporine. As for IMQ, cells purified at d14 p.i. did not upregulate IRF-5 (Figure 6A) or DR5 (Figure 6B) with any of the stimuli. Only IMQ and the supernatant of apoptotic splenocytes induced IRF-5 and DR5 expression 30 hr after incubation on CD4 T cells enriched at d21 and d28 p.i. (Figures 6A, 6B, S5A, and S5B). Similarly, only the incubation of CD4 T cells with IMQ and the SN of apoptotic splenocytes led to an increase in cell death (Figure 6C), and all other treatments did not alter the survival of the cells at any time point observed. This suggests that microbial sensing or TLR9 and 4 were not involved in inducing IRF-5 expression and cell death in CD4 T cells during VL, but this pathway was rather triggered by tissue disruption and TLR7.

Apoptotic Cell Material Induces IRF-5 via TLR7

Our results indicate that TLR7 and tissue disruption can both induce IRF-5 in CD4 T cells from *L. donovani*-infected mice. Hence, we next investigated whether the SN from apoptotic cells was inducing IRF-5 via TLR7. CD4 T cells were purified from *L. donovani*-infected C57BL/6 mice at d14 and d21 p.i. and incubated with medium alone, IMQ, or SN from apoptotic cells. Cells
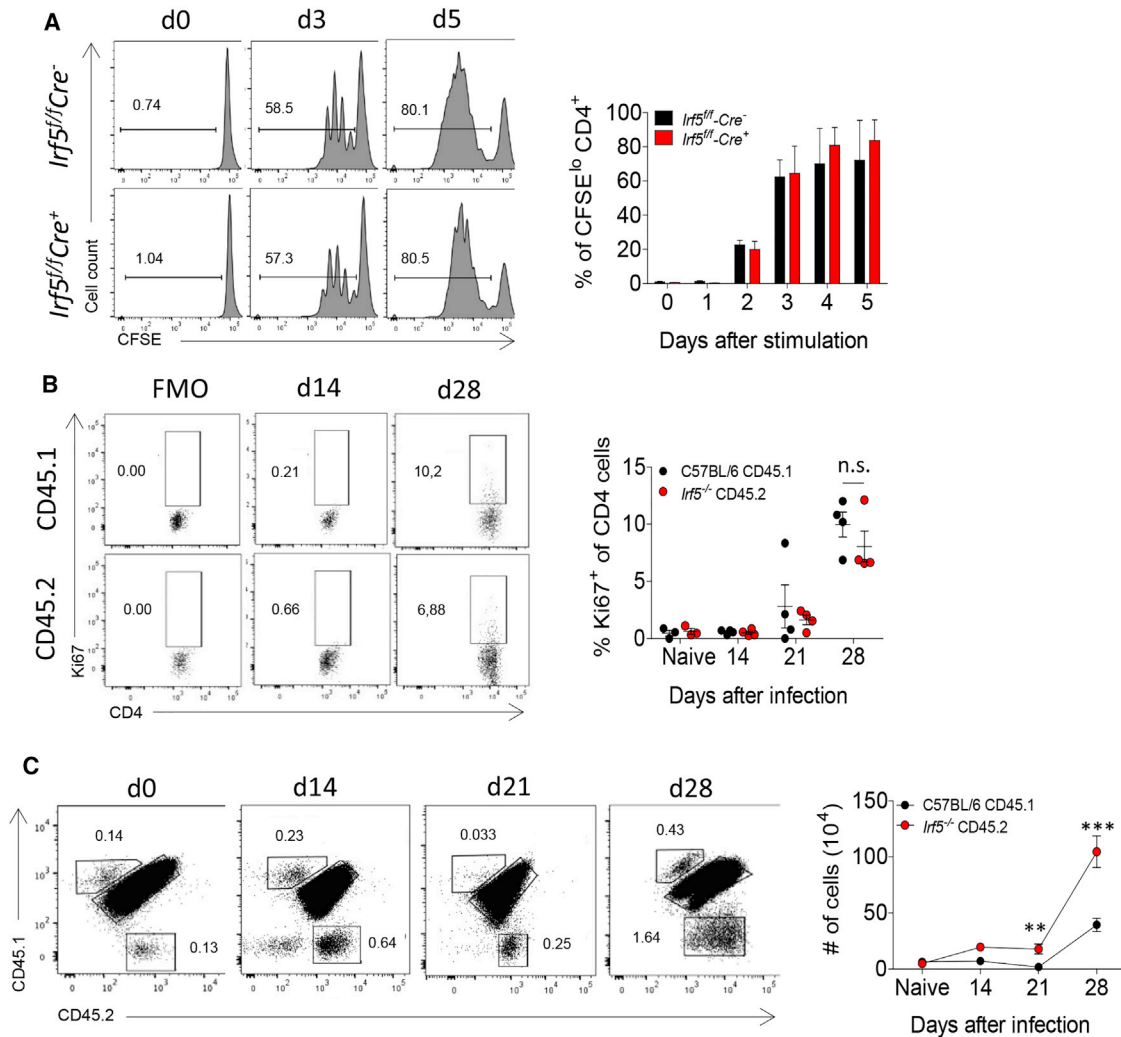

(G) Real-time PCR analysis of DR5 mRNA levels in CD4 T cells purified from the spleen of infected mice and incubated with medium or IMQ.

(H) Percentage of apoptotic CD4^+^ T cells in infected *Irf5*^*f/f*^-*Cre*^−^ or *Irf5*^*f/f*^-*Cre*^+^ mice.

(I) Apoptosis fold induction in splenic CD4 T cells from infected mice 30 hr after IMQ treatment. Apoptosis fold induction was calculated as follows: (cell death in IMQ treated sample − *ex vivo* cell death)/(medium control cell death − *ex vivo* cell death).

(J) Apoptosis fold induction in CD4 T cells from d21-infected mice following a 6-hr-incubation with recombinant TRAIL; fold induction was calculated as (cell death in rTRAIL treated sample − *ex vivo* cell death)/(medium control cell death − *ex vivo* cell death).

Data represent the mean ± SEM of one of 3 independent experiments; n = 4. *p < 0.05; **p < 0.01; ***p < 0.001.

Figure 5. IRF-5 Does Not Affect CD4 T Cell Proliferation during *L. donovani* Infection

(A) CFSE-labeled, IRF-5-sufficient, and -deficient CD4 T cells were stimulated with anti-CD3/CD28; CFSE dilution was used as readout for proliferation. Representative histograms (left panel) and percentages (right panel) of CFSE^{lo} CD4 T cells are shown.

(B and C) 5×10^6 CD45.1 C57BL/6 and *Irf5*$^{-/-}$ CD4 T cells were co-transferred into CD45.1/CD45.2 recipients a day prior to *L. donovani* infection. Mice were then euthanized at various time points after infection. (B) Representative dot plots (left panel) and percentages (right panel) of Ki67$^+$ CD4 T cells; (C) representative dot plots (left panel) and average numbers (right panel) of CD45.1 WT (*Irf5*$^{f/f}$-*Cre*$^-$) and CD45.2 *Irf5*-deficient (*Irf5*$^{f/f}$-*Cre*$^+$) CD4 T cells. Data represent the mean ± SEM. **p < 0.01; ***p < 0.001.
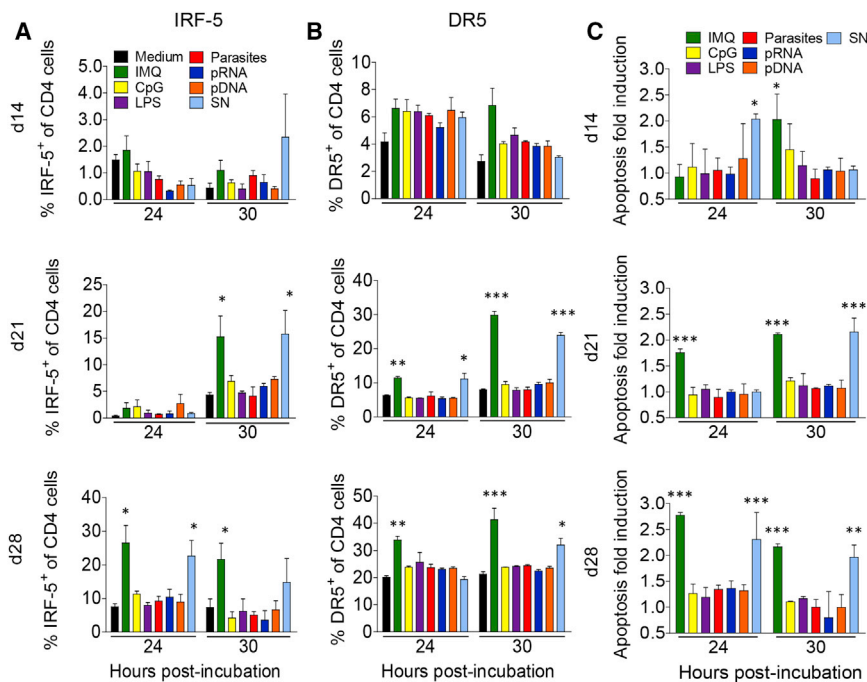
were also treated or not with synthetic oligodeoxynucleotides with immunoregulatory sequences (IRSs) that specifically block signaling via TLR7, IRS661 (Barrat et al., 2005). Thirty hours later, IRF-5 expression was assessed by Image Stream. As expected, IRF-5 induction following IMQ treatment of d21 p.i. CD4 T cells was inhibited by IRS661 (Figure 7A). Interestingly, the TLR7 antagonist also prevented the upregulation of IRF-5 following incubation of CD4 T cells purified at d21 p.i. with SN from staurosporine-treated cells (Figure 7A), suggesting that apoptotic material also signals via TLR7. No differences in the level of IRF5 expression were detected after any treatment of CD4 T cells purified at d14 p.i.

To identify the SN component(s) that triggers TLR7, we purified RNA and DNA (Figure S6) from the SN of apoptotic cells

and analyzed whether IRF-5 was induced by these two components. As expected, treatment of splenic *Cre*$^-$ CD4 T cells from d21-infected mice with IMQ or SN resulted in the upregulation of IRF-5 mRNA, which was abrogated by the TLR7 agonist IRS661 oligodeoxynucleotide (ODN) (Figure 7B). In contrast, IRF-5 mRNA levels did not change when RNA or DNA purified from the SN of apoptotic cells was added to the same *Cre*$^-$ CD4 T cells (Figure 7B), suggesting that pure RNA or DNA from apoptotic cell material is not involved in the TLR7-dependent IRF-5 induction in CD4 T cells.

Similarly to IRF-5, DR5 expression was also not induced following incubation of *Cre*$^-$ CD4 T cells with RNA or DNA purified from the SN of apoptotic cells, but it was induced, as expected, by IMQ and the SN in cells purified at d21 p.i. (Figure 7C).

Figure 6. TLR7-Mediated IRF-5 Activation and CD4 Cell Death Are Not a Consequence of Microbial Sensing

Mice were infected with 2×10^7 amastigotes intravenously and euthanized at various time points after infection. CD4 T cells were purified from the spleen of infected mice and incubated with medium, IMQ, CpG, LPS, living parasites (P), parasite RNA (pRNA), parasite DNA (pDNA), or supernatant from apoptotic cells (SN). Graphs show the percentage of splenic CD4 T cells from infected mice expressing (A) IRF5, (B) DR5, and (C) the fold induction of apoptosis in CD4 T cells from infected mice after treatments. Data represent the mean ± SEM of one of 3 independent experiments; n = 4. *p < 0.05; **p < 0.01; ***p < 0.001.
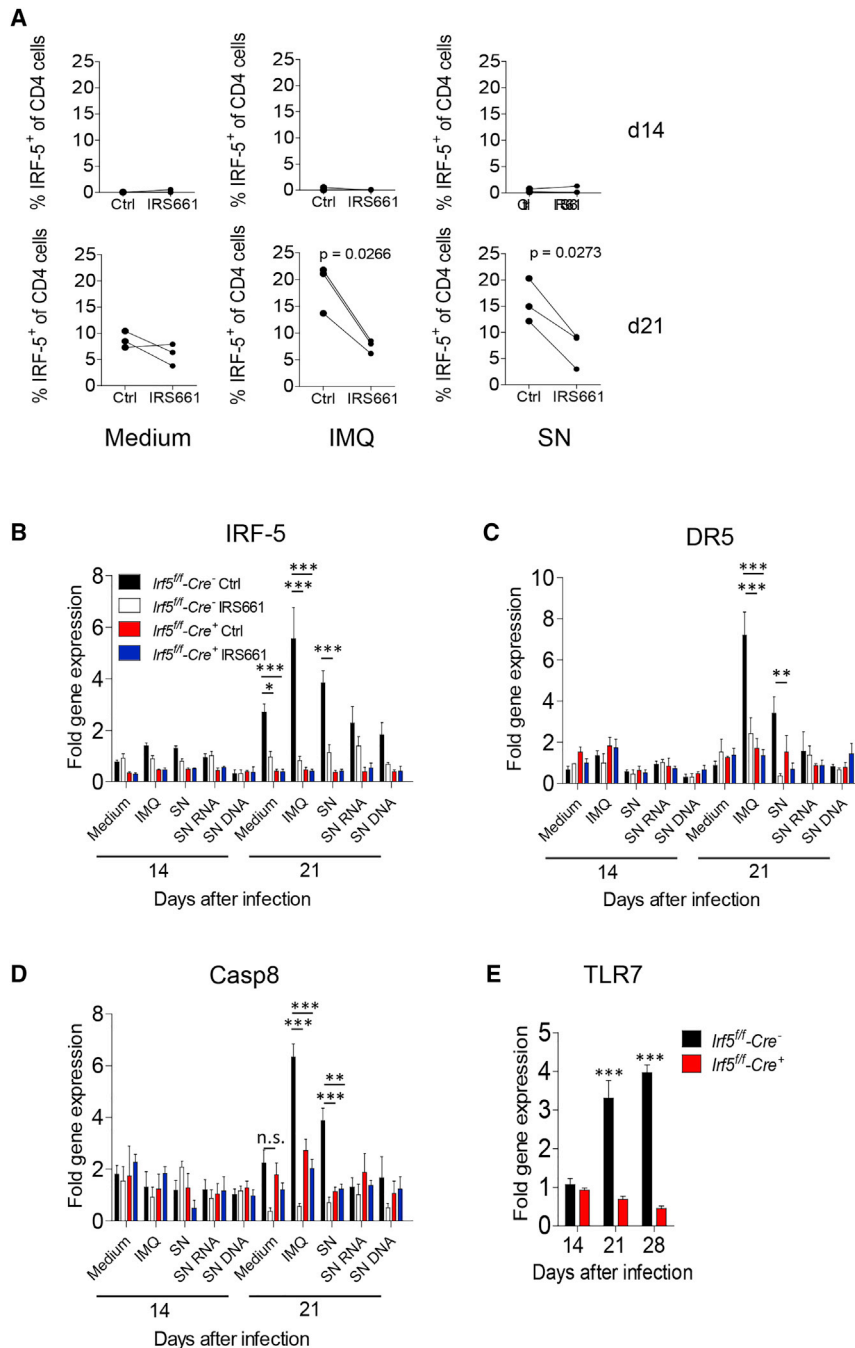
DISCUSSION

Chronic infections are typically associated with anti-inflammatory responses aimed at regulating T cell responses and limiting tissue injuries. However, these responses often favor pathogen persistence and may result in immune suppression. In the present study, we propose IRF-5 as an important player in the regulation of pro-inflammatory CD4 T cells. We show that TLR7-mediated IRF-5 activation is enhancing DR5-dependent induction of apoptosis of protective IFN-γ-producing CD4 T cells in *L. donovani*-infected mice. T-cell-specific IRF-5 ablation resulted in stronger IFN-γ responses and ultimately lower parasite burden. Our results also suggest that this pathway is triggered by tissue disruption.

Inflammation is essential for controlling intracellular pathogen growth. However, excessive and/or chronic inflammation often leads to tissue damage and initiates anti-inflammatory tissue-protecting pathways. In the case of VL, disruption of the splenic microarchitecture occurs from d14 p.i. on and leads to an impaired capacity of naive T cells and dendritic cells to migrate to T cell area (Ato et al., 2002) and a progressive loss of B cell germinal centers (Smelt et al., 1997). TNF is largely responsible for initiating this process as well as for inducing IL-10 (Ato et al., 2002; Engwerda et al., 2002). Tissue damage is accompanied by a massive infiltration of inflammatory cells and by splenomegaly (Hammami et al., 2017). In this environment, we observed a gradual upregulation and activation of IRF-5 in IFN-γ⁺ CD4 T cells. Increased IRF-5 expression was paralleled by an upregulation of TLR7 and DR5. Although high IFN-I levels have been linked to DR5 and lymphocytes death (Hardy et al., 2007; Herbeuval et al., 2006), we did not see a direct effect of IFN-I on IRF-5 upregulation and CD4 T cell death in *L. donovani*-infected mice. In contrast, IRF-5 appeared to be induced by TLR7. TLR9 and 4, which are both expressed in T cells (Rahman et al., 2009), do not seem to promote IRF-5 expression in CD4 T cells. The function of innate sensors in cells of adaptive immunity is still a fairly unexplored field. TLR signaling pathways in T cells were shown to be necessary for

Treatment with IRS661 ODN abrogated DR5 induction. To note, DR5 was not upregulated in CD4 from *Cre⁺* mice even when treated with IMQ and SN, confirming that IRF-5 is required in this pathway. We next determined the level of caspase 8 mRNA expression (Figure 7D). Caspase 8 is another reported downstream target of IRF-5 (Hu and Barnes, 2009) and is part of the TRAIL-mediated cell death signaling pathway. Treatment of CD4 T cells purified from d21-infected *Cre⁻* mice with IMQ or SN resulted in a significant caspase 8 induction, which was blocked by IRS661 ODN. No effect on caspase 8 mRNA expression levels was observed when the same cells were incubated with RNA or DNA purified from the SN of apoptotic cells (Figure 7D). As for DR5, *Cre⁻* CD4 T cells and IRF-5-deficient CD4 T cells purified from infected mice at d14 or d14 and d21 p.i., respectively, did not upregulate caspase 8 expression under any condition tested (Figure 7D). Taken together, our results suggest that RNA or DNA from staurosporine-treated cells cannot trigger TLR7 to induce IRF-5 in CD4 T cells and that IRF-5 is a crucial component in this pathway.

We finally sought to understand whether the lack of IRF-5 was somehow altering TLR7 expression on CD4 T cells, and this would additionally contribute to the reduced cell death observed in IRF-5-deficient CD4 T cells. To this end, we monitored TLR7 expression on CD4 T cells at d14, d21, and d28 p.i. in *L. donovani*-infected *Cre⁻* and *Cre⁺* mice. As shown before (Figure 4A), TLR7 expression was increasingly upregulated over the course of infection in *Cre⁻* CD4 T cells (Figure 7E). In contrast, TLR7 mRNA was maintained on a stable level in IRF-5-deficient CD4 T cells (Figure 7E), suggesting that IRF-5 is not only directly involved in the TLR7-IRF-5-DR5 pathway, but it also participates in a feedforward loop to upregulate TLR7 expression.

was the induction of IRF-5 and subsequently DR5, a known target of IRF-5 (Hu and Barnes, 2009). The TLR7-IRF-5 pathway was sensitizing CD4 T cells to TRAIL-mediated cell death. Interestingly, IRF-5 and DR5 were mainly expressed in IFN-γ$^+$ CD4 T cells, suggesting that induction of apoptosis via IRF-5 preferentially affected pro-inflammatory cells. This observation prompted us to believe that this pathway may be in place to protect inflammation-mediated tissue injuries.

A major question that arose during our study pertained to the nature of the ligand responsible for triggering TLR7 in CD4 T cells: is the TLR7 pathway activated following microbial sensing? *Leishmania* typically resides in parasitophorous vacuoles inside macrophages (Arango Duque et al., 2014). Although parasites have been seen inside or on various cells other than macrophages (Abidin et al., 2017; Bankoti et al., 2012; Ribeiro-Gomes et al., 2012; Romano et al., 2017; Silva-Barrios et al., 2016), they were never reported to be internalized by T cells. However, there is still the remote possibility though that dead parasites or RNA from dead parasites could be internalized by T cells and trigger TLR7. Our results refute this possibility: *Leishmania* or leishmanial DNA/RNA does not trigger TLR7 to induce IRF-5 in T cells, suggesting that IRF-5-induced cell death during VL is not a consequence of microbial sensing.

Because splenic tissue disruption is a characteristic feature of VL (Silva-Barrios et al., 2016) and, in SLE patients, IRF-5 can be induced by apoptotic and/or necrotic material (Stone et al., 2012), we were not surprised to observe that the supernatant of apoptotic splenocytes induced IRF-5 expression and consequently cell death of CD4 T cells from *L. donovani*-infected mice. Interestingly, RNA and DNA released by apoptotic cells were not involved in this induction, suggesting that other, yet

effective clonal expansion, in that they act synergistically with T cell receptor (TCR)-induced signals to enhance proliferation, survival, and cytokine production in effector cells (Rahman et al., 2009). Nevertheless, TLR7 was reported to induce anergy in human CD4 T cells (Dominguez-Villar et al., 2015). A similar antiproliferative activity was also recently attributed to stimulator of IFN genes (STING) in T lymphocytes (Cerboni et al., 2017). We also observed a reduction in proliferation of CD4 T cells from *L. donovani*-infected mice in the presence of IMQ (data not shown); however, the most remarkable effect of TLR7 triggering

unidentified supernatant components may trigger the TLR7 pathway in T cells. Hence, local tissue damage mediated by persistent inflammation leads to suppression of protective T cell responses during chronic VL. The fact that IRF-5 is not activated in hepatic CD4 T cells supports our conclusions. Indeed, this organ clears *L. donovani* infection by generating a very efficient granulomatous response without major disruption of the hepatic microarchitecture. It is well documented that dying cells can regulate adaptive immunity by the release of damage-associated molecular pattern (DAMP). However, DAMPs are mainly known for promoting inflammation and provide immunogenic signals enhancing T cell priming (Yatim et al., 2017). In our model of chronic infection, tissue damage appears to dampen pro-inflammatory CD4 T cell responses rather than promoting inflammation. This discrepancy probably depends on the cell and receptor recognizing DAMPs and on the stage of infection; innate sensors may have very different functions in T cells in a chronic inflammatory environment.

Although the activation of the TLR7-IRF-5-DR5 axis in T cells protects the spleen by reducing inflammation, it is also beneficial to the establishment of persistent *L. donovani* infection. Indeed, IFN-γ⁺ CD4 T cells are essential for controlling parasite growth during chronic VL (Engwerda et al., 1998). In *L. donovani*-infected mice, IFN-γ-producing CD4 T cells are first detectable at d14 p.i. and reach maximal expansion at d28 p.i. In the liver, high frequencies of parasite-specific IFN-γ⁺ CD4 T cells are observed (Paun et al., 2011); in contrast, small percentages of IFN-γ-producing CD4 T cells are typically detected in the spleen. Because progressive tissue damage and upregulation of TLR7 also occur during this time in the spleen, we believe that IRF-5-mediated CD4 T cell death severely undermines the expansion and, later, the maintenance of protective responses in this organ. This highlights a tissue-specific inhibition of CD4 T cell responses in *L. donovani*-infected mice. It remains to determine though whether IRF-5-mediated death of effector CD4 T cells is restricted to *Leishmania*-specific responses or extends to all effector CD4 T cells present in the spleen and therefore is accountable for the general immune suppression observed in VL patients.

Another observation that requires further investigation concerns the regulation of TLR7 expression in CD4 T cells. Our results indicate that IRF-5 is involved in the upregulation of this receptor. However, we do not yet know the exact role of IRF-5 in this feedforward loop or the initial signal(s) responsible for inducing and activating IRF-5. Because TLR7 is also upregulated on T cells during chronic viral infections in humans (Dominguez-Villar et al., 2015; Hammond et al., 2010), dissecting the dynamic of IRF-5 and TLR7 induction in T cells could help identify potential therapeutic targets aimed at reversing suppression of protective T cell responses during persistent infections.

In conclusion, we propose IRF-5 as an important player in the regulation of IFN-γ⁺ CD4 T cell responses during chronic VL. Activation of this transcription factor is TLR7 dependent and appears to be induced by apoptotic and/or necrotic material. In IFN-γ⁺ CD4 T cells, IRF-5 promotes the expression of DR5 and caspase 8, sensitizing these cells to TRAIL-mediated cell death. Because tissue disruption is a common characteristic of persistent infections, this regulatory pathway may not only be

activated during VL but could be a generalized mechanism present in other chronic infectious diseases.

EXPERIMENTAL PROCEDURES

Mice and Parasites

B6.129S7-*Rag1*^tm1Mom^ and congenic B6-Ly5.1 mice were purchased from The Jackson Laboratory. C57BL/Bl6-*Tlr7*^−/−^ mice and *Ifnar*^−/−^ mice were a kind gift from Drs. Alain Lamarre (INRS-Institut Armand Frappier) and Jörg Hermann Fritz (McGill University). Mice with a targeted IRF-5 mutation in T cells were generated by crossing *Irf5*^flox/flox^ mice (Hammami et al., 2015) with mice expressing the cre-recombinase under the Lck promoter. All mice were housed at the Institut National de la Recherche Scientifique (INRS) animal facility under specific pathogen-free conditions and used at 6–10 weeks of age. *Leishmania donovani* (strain LV9) were maintained by serial passage in B6.129S7-*Rag1*^tm1Mom^ mice, and amastigotes were isolated from the spleen of infected animals. Mice were infected by injecting 2 × 10⁷ amastigotes intravenously via the lateral tail vein. Splenic parasite burden was determined by examining methanol-fixed, Giemsa stained tissue impression smears. Data are presented as *Leishmania donovani* units (LDUs) (Silva-Barrios et al., 2016).

Study Approval

Experiments involving mice were carried out under protocols approved by the Comité Institutionnel de Protection des Animaux of the INRS-Institut Armand Frappier (1510-02 and 1602-02). These protocols respect procedure on good animal practice provided by the Canadian Council on Animal Care. No differences in the course of *L. donovani* infection were observed between male and female mice, so male and female mice were used indiscriminately. Nevertheless, male mice were always matched and compared to male mice for the various experimental groups.

In Vivo Th1 Polarization

CD4 T cells were enriched by magnetic cell sorting (MACS) using a CD4 T cell isolation kit (Miltenyi Biotech) and activated for 5 days with plate-bound 1 μg/mL anti-CD3 (clone 145-2C1C; eBioscience) and 2 μg/mL anti-CD28 (clone 37.51; eBioscience) in the presence of 2 ng/mL IL-2 and 30 ng/mL IL-12 (PeproTech). Cells were then restimulated for 4 hr with phorbol 12-myristate 13-acetate (PMA)/ionomycin in the presence of Brefeldin A (Sigma), harvested, and analyzed by flow cytometry as detailed below.

In Vitro CD4 T Cell Proliferation

CD4 T cells were enriched by MACS using a CD4 T cell isolation kit (Miltenyi Biotech) and then stained with CFSE as previously described (Joshi et al., 2009). CFSE-labeled CD4 T cells were activated with plate-bound 1 μg/mL anti-CD3 (clone 145-2C1C; eBioscience) and 2 μg/mL anti-CD28 (clone 37.51; eBioscience) in the presence of 2 ng/mL IL-2 and analyzed by flow cytometry as detailed below.

Adoptive Transfer Experiments

C57BL/6, C57BL/6-Ly5.1, *Irf5*^−/−^, *Tlr7*^−/−^, and *Ifnar*^−/−^ mice were used as CD4 T cells donors. CD4 T cells were enriched by MACS from splenocytes of naive animals using a CD4 T cell isolation kit (Miltenyi Biotech). 5 × 10⁶ donor CD4 T cells were injected into the lateral tail vein of congenic B6-Ly5.1 or B6-Ly5.1-Ly5.2 mice the day prior to infection with *L. donovani* amastigotes. Mice were sacrificed at the indicated time points.

Flow Cytometry

The following antibodies were used for surface staining: BV421-conjugated anti-CD3 (clone 145-2C11; BD Biosciences); BV421-conjugated anti-CD4 (clone GK1.5; BD Biosciences); fluorescein isothiocyanate (FITC)-conjugated anti-CD4 (clone GK1.5; BD Biosciences); phycoerythrin (PE)-conjugated anti-CD4 (clone GK1.5; BD Biosciences); FITC-conjugated anti-CD45.2 (clone 104; BD Biosciences); APC-conjugated anti-CD8 (clone 53-6.7; BD Biosciences); APC-conjugated streptavidin (BD Biosciences); APC-R700-conjugated anti-CD117 (clone 2B8; BD Biosciences); APC-conjugated annexin V (BD Biosciences); PE-conjugated anti-PD-1 (clone J43;

eBioscience); biotin-conjugated anti-DR5 (clone MD5.1; eBioscience); PE-conjugated anti-CD25 (clone PC61.5; eBioscience); PE-Cy7-conjugated anti-TIM3 (clone B8.2C12; BioLegend); PE-conjugated anti-Fas (clone SA367H8; BioLegend); APC-conjugated anti-CD120a (TNFR-I; clone 55R-286; BioLegend); BV650-conjugated CD45.2 (clone 104; BD Biosciences); and Zombie Aqua Fixable Viability Kit (BioLegend). Intracellular staining was performed as previously described (Hammami et al., 2015). Briefly, splenocytes were either restimulated with bone-marrow-derived dendritic cells (BMDCs) pulsed with fixed parasites or PMA/ionomycin in the presence of Brefeldin A (BD Biosciences). After fixation, cells were permeabilized and stained with the following antibodies: APC-conjugated anti-IFNγ (clone XMG1.2; BD Biosciences); PE-conjugated anti-IL-10 (BD Biosciences); AF488-conjugated anti-FoxP3 (clone FJK-16 s; eBioscience); PE-Cy7-conjugated anti-Ki67 (clone 16A8; BioLegend); and propidium iodide (Sigma). Flow cytometric analysis was performed with a BD LSRFortessa cell analyzer (Becton Dickinson). Samples were analyzed with Flowjo and DIVA software.

ImageStream Flow Cytometry

The following antibodies were used for surface staining: PE-conjugated anti-CD4 (clone GK1.5); biotin-conjugated anti-CD4 (clone GK1.5); biotin-conjugated anti-CD45.2 (clone 104; cat no. 553771); PE-Cy7-conjugated streptavidin; APC-conjugated streptavidin; PE-conjugated anti-CD62L (clone MEL-14); APC-conjugated anti-CD44 (clone IM7); and biotin-conjugated anti-CD3 (clone 145-2C11) from BD Biosciences. For intracellular staining, cells were stimulated with BMDCs pulsed with fixed parasites in the presence of Brefeldin A (BD Biosciences) and stained with surface antibodies. After fixation, cells were permeabilized and stained with APC-conjugated anti-IFN-γ (clone XMG1.2; BD Biosciences) and AF488-conjugated anti-IRF5 (R&D Systems). DAPI (Invitrogen) was used to stain the nucleus of cells immediately before acquisition. Samples were acquired using the ImageStreamX MKII flow cytometer and analyzed with IDEAS software (Amnis, Seattle, WA, USA). 200,000–500,000 gated cell singlets were analyzed for each sample. Nuclear localization of IRF5 was measured using a morphology mask to determine a similarity score, which quantifies the correlation of pixel values of the DAPI and IRF5 images on a per cell basis. A similarity score >1 was used as a cutoff for nuclear localization. Cells in individual bins were visually inspected to confirm subcellular localization (values < or >1).

Real-Time qPCR Analysis

RNA from isolated CD4 T cells from *in vitro* or *in vivo* experiments was extracted using the RNeasy mini kit (QIAGEN) as per manufacturer's instructions. Reverse transcription was carried out using the iScript cDNA synthesis kit (Bio-Rad) as previously described (Hammami et al., 2015). Real-time PCR analysis was performed using iTaq Universal SYBR Green Supermix (Bio-Rad). *Dr5*, *Irf5*, *Tlr7*, and *Hprt* were amplified using the following primers: *Hprt*, 5′-GTT GGA TAC AGG CCA GAC TTT GTT G-3′ and 5′-GAT TCA ACC TTG CGC TCA TCT TAG GC-3′; *Tnfrsf10b* (*DR5*), 5′-TGA CGG GGA AGA GGA ACT GA-3′ and 5′-GGC TTT GAC CAT TTG GAT TTG-3′; *Irf5*, 5′-TAG AGG CTA CCC AGG AGC AA-3′ and 5′-GCC CAC TCC AGA ACA CCT TA-3′; *Tlr7*, 5′-GGC ATT CCC ACT AAC ACC AC-3′ and 5′-TTG GAC CCC AGT AGA ACA GG-3′; and *Casp8*, 5′-CTC CGA AAA ATG AAG GAC AGA-3′ and 5′-CGT GGG ATA GGA TAC AGC AGA-3′. All PCRs were carried out with the Stratagene mx3000P real-time PCR system. Data were normalized to hypoxanthine-guanine phosphoribosyltransferase (HPRT) and expressed as fold gene regulation compared to naive controls.

In Vitro CD4 T Cell Stimulation and Recombinant TRAIL Treatment

CD4 T cells were purified following manufacturer's instructions from splenocytes of infected and naive mice using a CD4 isolation kit (Miltenyi Biotech). Purified CD4 T cells (purity >95%) were incubated at 37°C for 24 hr or 30 hr with 5 μg/mL imiquimod (Invivogen), 3 μg/mL CpG (Invivogen), 10 μg/mL LPS (Sigma), amastigotes at a MOI of 1:10, 500 ng/mL parasite RNA, 500 ng/mL parasite DNA, 10% v/v supernatant of staurosporine-treated cells, 500 ng/mL RNA, or 500 ng/mL DNA purified from supernatant of staurosporine-treated cells. ODNs IRS661 (5′-TGCTTGCAAGCTTGCAAGCA-3′) were used as TLR7 antagonist; 5′-TCCTGCAGGTTAAGT-3′ ODNs were used as control (Barrat et al., 2005). ODNs were prepared in sterile water

and utilized at 5.6 μg/mL. Cells were treated with IRS661 30 min before to receive other treatments. For TRAIL treatment, CD4 T cells were purified as mentioned above and incubated at 37°C for 6 hr with 100 ng/mL recombinant murine TRAIL (Peprotech). Cells were cultured in RPMI-1640 (Gibco; Invitrogen) supplemented with 10% fetal bovine serum (FBS).

Statistical Analysis

Statistical analysis was performed using paired Student's t test or multi-way ANOVA. Statistical analysis was conducted using Graphpad Prism (GraphPad). Differences were considered to be statistically significant when p < 0.05. All experiments were conducted independently at least three times.

AUTHOR CONTRIBUTIONS

A.F. performed experiments, analyzed data, and wrote the manuscript; S.S. conceived the project, designed the experimental approach, interpreted data, and wrote the manuscript; X.D.-L. performed experiments; L.T.M. and A.H. performed experiments and analyzed data; and J.v.G. provided key expertise and interpreted data.

DECLARATION OF INTERESTS

The authors declare no competing interests.

REFERENCES

Abidin, B.M., Hammami, A., Stäger, S., and Heinonen, K.M. (2017). Infection-adapted emergency hematopoiesis promotes visceral leishmaniasis. PLoS Pathog. *13*, e1006422.

Arango Duque, G., Fukuda, M., Turco, S.J., Stäger, S., and Descoteaux, A. (2014). Leishmania promastigotes induce cytokine secretion in macrophages through the degradation of synaptotagmin XI. J. Immunol. *193*, 2363–2372.

Ato, M., Stäger, S., Engwerda, C.R., and Kaye, P.M. (2002). Defective CCR7 expression on dendritic cells contributes to the development of visceral leishmaniasis. Nat. Immunol. *3*, 1185–1191.

Bankoti, R., and Stäger, S. (2012). Differential regulation of the immune response in the spleen and liver of mice infected with Leishmania donovani. J. Trop. Med. *2012*, 639304.

Bankoti, R., Gupta, K., Levchenko, A., and Stäger, S. (2012). Marginal zone B cells regulate antigen-specific T cell responses during infection. J. Immunol. *188*, 3961–3971.

Barnes, B.J., Moore, P.A., and Pitha, P.M. (2001). Virus-specific activation of a novel interferon regulatory factor, IRF-5, results in the induction of distinct interferon alpha genes. J. Biol. Chem. *276*, 23382–23390.

Barnes, B.J., Kellum, M.J., Pinder, K.E., Frisancho, J.A., and Pitha, P.M. (2003). Interferon regulatory factor 5, a novel mediator of cell cycle arrest and cell death. Cancer Res. *63*, 6424–6431.

Barnes, B.J., Richards, J., Mancl, M., Hanash, S., Beretta, L., and Pitha, P.M. (2004). Global and distinct targets of IRF-5 and IRF-7 during innate response to viral infection. J. Biol. Chem. *279*, 45194–45207.

Barrat, F.J., Meeker, T., Gregorio, J., Chan, J.H., Uematsu, S., Akira, S., Chang, B., Duramad, O., and Coffman, R.L. (2005). Nucleic acids of mammalian origin can act as endogenous ligands for Toll-like receptors and may promote systemic lupus erythematosus. J. Exp. Med. *202*, 1131–1139.

Bi, X., Feng, D., Korczeniewska, J., Alper, N., Hu, G., and Barnes, B.J. (2014). Deletion of Irf5 protects hematopoietic stem cells from DNA damage-induced apoptosis and suppresses γ-irradiation-induced thymic lymphomagenesis. Oncogene *33*, 3288–3297.

Caramalho, I., Lopes-Carvalho, T., Ostler, D., Zelenay, S., Haury, M., and Demengeot, J. (2003). Regulatory T cells selectively express toll-like receptors and are activated by lipopolysaccharide. J. Exp. Med. *197*, 403–411.

Cerboni, S., Jeremiah, N., Gentili, M., Gehrmann, U., Conrad, C., Stolzenberg, M.C., Picard, C., Neven, B., Fischer, A., Amigorena, S., et al. (2017). Intrinsic antiproliferative activity of the innate sensor STING in T lymphocytes. J. Exp. Med. *214*, 1769–1785.

Couzinet, A., Tamura, K., Chen, H.M., Nishimura, K., Wang, Z., Morishita, Y., Takeda, K., Yagita, H., Yanai, H., Taniguchi, T., and Tamura, T. (2008). A cell-type-specific requirement for IFN regulatory factor 5 (IRF5) in Fas-induced apoptosis. Proc. Natl. Acad. Sci. USA *105*, 2556–2561.

Dideberg, V., Kristjansdottir, G., Milani, L., Libioulle, C., Sigurdsson, S., Louis, E., Wiman, A.C., Vermeire, S., Rutgeerts, P., Belaiche, J., et al. (2007). An insertion-deletion polymorphism in the interferon regulatory Factor 5 (IRF5) gene confers risk of inflammatory bowel diseases. Hum. Mol. Genet. *16*, 3008–3016.

Dieguez-Gonzalez, R., Calaza, M., Perez-Pampin, E., de la Serna, A.R., Fernandez-Gutierrez, B., Castañeda, S., Largo, R., Joven, B., Narvaez, J., Navarro, F., et al. (2008). Association of interferon regulatory factor 5 haplotypes, similar to that found in systemic lupus erythematosus, in a large subgroup of patients with rheumatoid arthritis. Arthritis Rheum. *58*, 1264–1274.

Dominguez-Villar, M., Gautron, A.S., de Marcken, M., Keller, M.J., and Hafler, D.A. (2015). TLR7 induces anergy in human CD4(+) T cells. Nat. Immunol. *16*, 118–128.

Engwerda, C.R., Murphy, M.L., Cotterell, S.E., Smelt, S.C., and Kaye, P.M. (1998). Neutralization of IL-12 demonstrates the existence of discrete organ-specific phases in the control of Leishmania donovani. Eur. J. Immunol. *28*, 669–680.

Engwerda, C.R., Ato, M., Cotterell, S.E., Mynott, T.L., Tschannerl, A., Gorak-Stolinska, P.M., and Kaye, P.M. (2002). A role for tumor necrosis factor-alpha in remodeling the splenic marginal zone during Leishmania donovani infection. Am. J. Pathol. *161*, 429–437.

Fukata, M., Breglio, K., Chen, A., Vamadevan, A.S., Goo, T., Hsu, D., Conduah, D., Xu, R., and Abreu, M.T. (2008). The myeloid differentiation factor 88 (MyD88) is required for CD4+ T cell effector function in a murine model of inflammatory bowel disease. J. Immunol. *180*, 1886–1894.

Gelman, A.E., Zhang, J., Choi, Y., and Turka, L.A. (2004). Toll-like receptor ligands directly promote activated CD4+ T cell survival. J. Immunol. *172*, 6065–6073.

Graham, R.R., Kozyrev, S.V., Baechler, E.C., Reddy, M.V., Plenge, R.M., Bauer, J.W., Ortmann, W.A., Koeuth, T., González Escribano, M.F., Pons-Estel, B., et al.; Argentine and Spanish Collaborative Groups (2006). A common haplotype of interferon regulatory factor 5 (IRF5) regulates splicing and expression and is associated with increased risk of systemic lupus erythematosus. Nat. Genet. *38*, 550–555.

Hammami, A., Charpentier, T., Smans, M., and Stäger, S. (2015). IRF-5-Mediated Inflammation Limits CD8+ T Cell Expansion by Inducing HIF-1α and Impairing Dendritic Cell Functions during Leishmania Infection. PLoS Pathog. *11*, e1004938.

Hammami, A., Abidin, B.M., Charpentier, T., Fabié, A., Duguay, A.P., Heinonen, K.M., and Stäger, S. (2017). HIF-1α is a key regulator in potentiating suppressor activity and limiting the microbicidal capacity of MDSC-like cells during visceral leishmaniasis. PLoS Pathog. *13*, e1006616.

Hammond, T., Lee, S., Watson, M.W., Flexman, J.P., Cheng, W., Fernandez, S., and Price, P. (2010). Toll-like receptor (TLR) expression on CD4+ and CD8+ T-cells in patients chronically infected with hepatitis C virus. Cell. Immunol. *264*, 150–155.

Hardy, A.W., Graham, D.R., Shearer, G.M., and Herbeuval, J.P. (2007). HIV turns plasmacytoid dendritic cells (pDC) into TRAIL-expressing killer pDC and down-regulates HIV coreceptors by Toll-like receptor 7-induced IFN-alpha. Proc. Natl. Acad. Sci. USA *104*, 17453–17458.

Herbeuval, J.P., Nilsson, J., Boasso, A., Hardy, A.W., Kruhlak, M.J., Anderson, S.A., Dolan, M.J., Dy, M., Andersson, J., and Shearer, G.M. (2006). Differential expression of IFN-alpha and TRAIL/DR5 in lymphoid tissue of progressor versus nonprogressor HIV-1-infected patients. Proc. Natl. Acad. Sci. USA *103*, 7000–7005.

Hu, G., and Barnes, B.J. (2009). IRF-5 is a mediator of the death receptor-induced apoptotic signaling pathway. J. Biol. Chem. *284*, 2767–2777.

Joshi, T., Rodriguez, S., Perovic, V., Cockburn, I.A., and Stäger, S. (2009). B7-H1 blockade increases survival of dysfunctional CD8(+) T cells and confers protection against Leishmania donovani infections. PLoS Pathog. *5*, e1000431.

Kaye, P.M., Svensson, M., Ato, M., Maroof, A., Polley, R., Stager, S., Zubairi, S., and Engwerda, C.R. (2004). The immunopathology of experimental visceral leishmaniasis. Immunol. Rev. *201*, 239–253.

Krausgruber, T., Blazek, K., Smallie, T., Alzabin, S., Lockstone, H., Sahgal, N., Hussell, T., Feldmann, M., and Udalova, I.A. (2011). IRF5 promotes inflammatory macrophage polarization and TH1-TH17 responses. Nat. Immunol. *12*, 231–238.

Oka, S., Mori, N., Matsuyama, S., Takamori, Y., and Kubo, K. (2000). Presence of B220 within thymocytes and its expression on the cell surface during apoptosis. Immunology *100*, 417–423.

Park, S., Murray, D., John, B., and Crispe, I.N. (2002). Biology and significance of T-cell apoptosis in the liver. Immunol. Cell Biol. *80*, 74–83.

Paun, A., Bankoti, R., Joshi, T., Pitha, P.M., and Stäger, S. (2011). Critical role of IRF-5 in the development of T helper 1 responses to Leishmania donovani infection. PLoS Pathog. *7*, e1001246.

Rahman, A.H., Taylor, D.K., and Turka, L.A. (2009). The contribution of direct TLR signaling to T cell responses. Immunol. Res. *45*, 25–36.

Ranatunga, D., Hedrich, C.M., Wang, F., McVicar, D.W., Nowak, N., Joshi, T., Feigenbaum, L., Grant, L.R., Stäger, S., and Bream, J.H. (2009). A human IL10 BAC transgene reveals tissue-specific control of IL-10 expression and alters disease outcome. Proc. Natl. Acad. Sci. USA *106*, 17123–17128.

Renno, T., Attinger, A., Rimoldi, D., Hahne, M., Tschopp, J., and MacDonald, H.R. (1998). Expression of B220 on activated T cell blasts precedes apoptosis. Eur. J. Immunol. *28*, 540–547.

Ribeiro-Gomes, F.L., Peters, N.C., Debrabant, A., and Sacks, D.L. (2012). Efficient capture of infected neutrophils by dendritic cells in the skin inhibits the early anti-leishmania response. PLoS Pathog. *8*, e1002536.

Romano, A., Carneiro, M.B.H., Doria, N.A., Roma, E.H., Ribeiro-Gomes, F.L., Inbar, E., Lee, S.H., Mendez, J., Paun, A., Sacks, D.L., and Peters, N.C. (2017). Divergent roles for Ly6C+CCR2+CX3CR1+ inflammatory monocytes during primary or secondary infection of the skin with the intra-phagosomal pathogen Leishmania major. PLoS Pathog. *13*, e1006479.

Schoenemeyer, A., Barnes, B.J., Mancl, M.E., Latz, E., Goutagny, N., Pitha, P.M., Fitzgerald, K.A., and Golenbock, D.T. (2005). The interferon regulatory factor, IRF5, is a central mediator of toll-like receptor 7 signaling. J. Biol. Chem. *280*, 17005–17012.

Silva-Barrios, S., Smans, M., Duerr, C.U., Qureshi, S.T., Fritz, J.H., Descoteaux, A., and Stäger, S. (2016). Innate Immune B Cell Activation by Leishmania donovani Exacerbates Disease and Mediates Hypergammaglobulinemia. Cell Rep. *15*, 2427–2437.

Smelt, S.C., Engwerda, C.R., McCrossen, M., and Kaye, P.M. (1997). Destruction of follicular dendritic cells during chronic visceral leishmaniasis. J. Immunol. *158*, 3813–3821.

Stäger, S., Maroof, A., Zubairi, S., Sanos, S.L., Kopf, M., and Kaye, P.M. (2006). Distinct roles for IL-6 and IL-12p40 in mediating protection against Leishmania donovani and the expansion of IL-10+ CD4+ T cells. Eur. J. Immunol. *36*, 1764–1771.

Stone, R.C., Feng, D., Deng, J., Singh, S., Yang, L., Fitzgerald-Bocarsly, P., Eloranta, M.L., Rönnblom, L., and Barnes, B.J. (2012). Interferon regulatory factor 5 activation in monocytes of systemic lupus erythematosus patients is triggered by circulating autoantigens independent of type I interferons. Arthritis Rheum. *64*, 788–798.

Takaoka, A., Yanai, H., Kondo, S., Duncan, G., Negishi, H., Mizutani, T., Kano, S., Honda, K., Ohba, Y., Mak, T.W., and Taniguchi, T. (2005). Integral role of IRF-5 in the gene induction programme activated by Toll-like receptors. Nature *434*, 243–249.

Tomita, T., Kanai, T., Fujii, T., Nemoto, Y., Okamoto, R., Tsuchiya, K., Totsuka, T., Sakamoto, N., Akira, S., and Watanabe, M. (2008). MyD88-dependent pathway in T cells directly modulates the expansion of colitogenic CD4+ T cells in chronic colitis. J. Immunol. *180*, 5291–5299.

Yatim, N., Cullen, S., and Albert, M.L. (2017). Dying cells actively regulate adaptive immune responses. Nat. Rev. Immunol. *17*, 262–275.